



ELSEVIER

Nuclear Physics A682 (2001) 320c–331c

www.elsevier.nl/locate/npe

Single-nucleon knockout reactions at fragmentation beam energies

J. A. Tostevin*

Department of Physics, School of Physics and Chemistry, University of Surrey,
Guildford, Surrey, GU2 7XH, United Kingdom

Single-nucleon knockout reactions show considerable promise as a spectroscopic tool for mapping the migration of the dominant single-particle strength in rare isotopes, produced as fragmentation beams with energies > 40 MeV/nucleon. In this paper the theoretical assumptions which underpin the eikonal theory treatment of these reactions are reviewed. Certain sensitivities to input parameters are discussed, as are the possible importance of classes of higher order corrections. The eikonal model prediction for the elastic breakup component of the nucleon removal cross sections is also compared with that from fully-quantum mechanical calculations using the discretised continuum coupled channels method. An asymmetry, manifest in the experimental longitudinal momentum distributions of the ground state residues in weakly-bound-nucleon removal, is well reproduced.

1. INTRODUCTION

An ability to map the evolution of the positions and order of nuclear single particle states in rare nuclei of high isospin will be an important component in developing our understanding and the reliability of structure models in these regions. The low intensities of secondary beams of these species, combined with the small number of excited states available in lighter systems, mean that conventional (but in inverse kinematics) light-ion single-nucleon transfer reaction and gamma spectroscopic methods are non-trivial. Nucleon-knockout reactions appear to offer an alternative and complementary technique which is particularly well adapted for rare isotope beams produced using fragmentation.

From a reaction theory point of view, it has been extremely fortuitous that many of the first generation facilities for the production of rare unstable nuclei have been based on nuclear fragmentation. The high secondary beam energies, and fast collisions with a secondary target, have allowed a rapid development and application of reaction methods, based on the sudden/adiabatic and/or eikonal-like approximations [1–8]. These lead to considerable simplifications and also practical and accurate calculation schemes which have relatively simple and physically transparent input parameters. This has allowed new experimental results to gain feedback rapidly from theory, and vice versa.

Having said this, very little of the extensive literature to date has discussed possible schemes to obtain detailed spectroscopic information from data. To a large extent,

*The financial support of the United Kingdom Engineering and Physical Sciences Research Council (EPSRC) in the form of Grants Nos. GR/J95867 and GR/M82141 is gratefully acknowledged

analyses have been used to gain confidence in the reaction methods, to try to identify unambiguously exotic and halo systems, e.g. to determine their sizes and possible dominant ground state configurations of valence nucleons. Additionally much effort has been aimed at few-body structure models of one- and two-neutron halo nuclei and their assessment, e.g. the role of correlations, using reaction calculations. A confidence has developed in the accuracy and the predictive power of eikonal (impact parameter based) reaction methods with, in general, good agreement between different approaches. The physical factors which influence the calculation of fragment cross sections and momentum distributions, such as core shadowing [9], are now well understood.

2. KNOCKOUT REACTIONS

In nucleon knockout reactions, events in which a single nucleon is removed from the incident (mass $A + 1$) nucleus by a light absorptive nuclear target (typically ${}^9\text{Be}$) are identified by detection of the residual or core nuclei c , of mass A , travelling with a velocity close to that of the incident beam. Since *only* the heavy projectile residue is detected, and not the state of the removed nucleon, the measurement is actually a highly inclusive one. It is the (incoherent) sum of (i) the cross sections for all processes in which the removed nucleon excites the target and is absorbed, called stripping, and (ii) the cross section for elastic breakup of the projectile, the target remaining in its ground state, called diffractive dissociation. Both of these processes must therefore be calculated and cannot be individually identified from the measurement of the residue. It is known however that the core angular distribution, the cross section as a function of the component of the residue's momentum perpendicular to the beam direction, does include such information.

The use of a nuclear rather than a nucleon target is crucial to introduce spatial localisation of the reaction at the nuclear surface. ${}^9\text{Be}$ in particular, with no bound excited states, essentially presents a black absorptive disk to the incident core of nucleons. The requirement of core survival, at near to beam velocity, dictates that those contributing core-target interactions are highly peripheral with the result that the removed nucleon's wave function is probed at and beyond the surface of the projectile [10]. This is then very similar to the situation in low-energy light-ion transfer reactions on medium mass nuclei where the short mean-free-paths of the ions lead to surface localisation [11].

The really powerful recent development, from a spectroscopy point of view, is the experimental capability to identify not only the core residue and its momentum but also its state ϕ^c by coincident detection of in-flight decay photons. The cross sections for producing the core fragment in excited states are now known to be very significant [12,13], even for halo nuclei where the projectile has a very weakly bound valence nucleon moving relative to the ground state of the core nucleons as a dominant configuration. This makes interpretation of (core state) inclusive measurements difficult, even for their dominant ground state structures. There are readily observable cross sections from the removal of the more-bound core nucleons. Reaction and structure theory are then required to interpret these different core state differential (momentum distributions) and integrated cross sections in terms of the single-particle spectroscopy - the orbital angular momentum ℓ and spectroscopic factor of the removed nucleon configuration. The former is determined by the width of the measured momentum distribution and the latter by the magnitude of

the integrated partial cross section to a given core state.

The technique discussed here has recently been applied in a number of important novel and test cases, $^{26,27,28}\text{P}$ [14], $^{11,12}\text{Be}$ [13,15,16], $^{13,14}\text{B}$ [17], and the neutron-rich carbon isotopes $^{15,16,17,19}\text{C}$ [18,19], to which the reader is referred. These are also reviewed by Hansen and Maddalena at this meeting. The analyses show a high degree of agreement between the deduced spectroscopy and that predicted by the shell-model. This paper clarifies the assumptions made in the reaction theory used, to date, in such studies. In a related recent systematic study, but in which the core state is not identified, the quality of agreement of the predictions of the method with inclusive (with respect to the core state) data on a wide range of psd-shell nuclei [20] adds to one's confidence in the basis of the method for extracting strong single particle strengths. A related picture was used earlier by Sagawa and Yazaki [21] to interpret the measured inclusive transverse momentum distribution of ^{10}Be fragments from ^{11}Be .

3. SPECTATOR CORE EIKONAL MODEL

The basis of the nucleon knockout calculations studied here has much in common with that of the distorted waves Born approximation (DWBA) treatment of single nucleon transfer reactions [11]. Earlier discussions of the accuracy and leading corrections to DWBA are highly relevant. Inherent in analyses of both knockout and transfer reaction data, is a need to learn the extent to which the intensities of the core states ϕ^c measured following the reaction reflect a pre-existing component in the incident projectile wave function. Alternatively, how important are (higher-order) dynamical processes which result in the outgoing flux being redistributed between core states by the reaction itself. We are not yet in a position to answer this question but we expect, and examples already show, that corrections will be significant in very weak transitions.

Here it is assumed that there *are* pre-formed components in the ground state wave function of the incident $A + 1$ -body projectile in which A of the nucleons are in state ϕ^c , and which can therefore be accessed by a single-nucleon knockout. Inelastic excitation of the state of these A nucleons is excluded in the reaction mechanism and is neglected in any final state interactions of the core with the target or with the removed nucleon. It follows that the reaction mechanism reduces to an effective three-body (nucleon+core+target) problem in which the core is a spectator particle which can therefore interact at most elastically with the target. This is expected to be a good starting point for low lying states of the $A + 1$ system with strong core state parentage. In common with other spectroscopic methods, for weakly populated ϕ^c , and core states with only small parentage in the projectile ground state, higher order dynamical effects are likely to be more significant. We return to this point briefly later.

Given the above, the projectile structure enters the reaction as in a single-nucleon transfer reaction, through the $\langle \phi^c | \Phi_{A+1} \rangle$ overlaps, and the cross section $\sigma(c)$ for populating a given core state c is

$$\sigma(c) = \sum C^2 S(c, n\ell j) \sigma_{sp}(S_n, n\ell j). \quad (1)$$

Here $C^2 S$ is the spectroscopic factor for the removal of a nucleon with given single-particle quantum numbers $(n\ell j)$, and expresses the parentage of this configuration in the initial

state with respect to the specific state c of the remaining nucleons. The sum must be taken over all non-vanishing configurations. The σ_{sp} are the single-particle removal cross sections from stripping and diffraction mechanisms, $\sigma_{sp} = \sigma_{sp}(str) + \sigma_{sp}(diff)$, discussed in the following. These are strongly ℓ - and nucleon separation energy S_n -dependent. It is implicit in Eq. (1) that the total angular momentum of the nucleon j and core c couple to that of the projectile ground state I , $I = c + j$.

4. EIKONAL STRIPPING CROSS SECTION

The nucleon stripping contribution to the cross section, $\sigma_{sp}(str)$, was elucidated formally by Hussein and McVoy [22] in the spectator core model and an expression given within the eikonal limit. This represents essentially the only practical way to calculate this cross section component, inclusive with respect to target excitation. A comprehensive review of the available fully-quantum mechanical formalisms has been given by Ichimura [23]. The eikonal expression takes the particularly intuitive form [22]

$$\sigma_{sp}(str) = \frac{1}{2I+1} \int d\mathbf{b} \sum_M \langle \phi_{IM}^c | (1 - |\mathcal{S}_n|^2) |\mathcal{S}_c|^2 | \phi_{IM}^c \rangle. \quad (2)$$

Here \mathcal{S}_c and \mathcal{S}_n are the elastic profile functions, the S-matrices of the core-target and removed nucleon-target systems expressed as functions of their impact parameters. Eq. (2) is then the integral over all projectile centre of mass impact parameters, and the average over M substates, of the product of the probabilities that the residue survives the reaction (in $|\mathcal{S}_c|^2$) but that the nucleon is absorbed (in $(1 - |\mathcal{S}_n|^2)$).

The removed nucleon-core relative motion wave functions $|\phi_{IM}^c\rangle$, or formfactors, are calculated in a Woods-Saxon potential well. For use with shell model spectroscopic factors, this well has standard radius and diffuseness parameters 1.25 and 0.7 fm and the depth of the potential is adjusted to reproduce the physical separation energy of the nucleon in the (initial) state, with a given $n\ell j$, from the core partition of interest. Alternatively one can use a formfactor and spectroscopy from another source, such as from few-body core-nucleon model calculations [16]. Calculations based on a defined two-body effective binding interaction allow a more consistent treatment of the eikonal diffraction dissociation cross section, as is discussed in the next section. The published analyses to date [14–19] have made almost exclusive use of shell model theory so as to provide a consistent treatment of all the core-nucleon configurations involved.

For compact, tightly bound, cores the \mathcal{S}_c have been calculated using the optical limit of Glauber theory [1]. The input parameters in the calculation are then an effective nucleon-nucleon interaction and the assumed nuclear matter distributions for the core and target nuclei. The effective interaction used is assumed to be a Gaussian [13] with an interaction range of 0.5 fm. This was chosen so that the \mathcal{S}_c calculate reaction cross sections consistent with known values for several nucleus-nucleus systems [24] at energies in the range 50–100 MeV/nucleon.

In some cases, however, such as p-wave core neutron removal from ^{11}Be , leaving ^{10}Be in the 1^- or 2^- states at about 6 MeV excitation [15], or in neutron removal from ^{12}Be [16] populating the $1/2^+$ ground state or $1/2^-$ state of ^{11}Be , the residue is itself an effective two-body core (b) plus nucleon system in which the nucleon is weakly bound and

delocalized. This few-body composite structure of the residue is then taken into account explicitly in determining the residue-target effective interaction and the appropriate \mathcal{S}_c [13], and

$$\mathcal{S}_c(b_c) = \langle \phi^b | \mathcal{S}_b \mathcal{S}_n | \phi^b \rangle \quad (3)$$

where ϕ^b describes the b -nucleon relative motion. Such an approach might also be applied to compute the stripping to an unbound state of the residue.

Generally speaking, the \mathcal{S}_c are highly absorptive, reflecting the accuracy of the black disk approximation to nucleus-nucleus collisions at the energies of interest. The \mathcal{S}_c essentially convey information on a lower impact parameter cutoff for the survival of the core fragment in the collision. This black-disc approximation is used in calculating the momentum distributions of the fragments [9] and is very accurate. There is a residual sensitivity in the details of the cross section calculations to using the more realistic \mathcal{S} , specifically to the choice of \mathcal{S}_n . This is clarified in a later Section.

5. EIKONAL ELASTIC BREAKUP CROSS SECTION

In the spectator eikonal model discussed here, the cross section for the elastic breakup of the projectile, integrated over all continuum final states of the core and nucleon with asymptotic spin projections μ and σ and relative wavenumber \mathbf{k} , is

$$\sigma_{sp}(diff) = \frac{1}{2I+1} \int d\mathbf{k} \int d\mathbf{b} \sum_{M\sigma\mu} |\langle \phi_{\sigma\mu}^{(-)}(c, \mathbf{k}) | \mathcal{S}_c \mathcal{S}_n | \phi_{IM}^c \rangle|^2. \quad (4)$$

The nucleon spin is s . The assumed spectator core is manifest by the fixed, and diagonal, nature of the core configuration in \mathcal{S}_c and the final state, a scattering state of the nucleon+core system in the presence of the interaction used to bind ϕ_{IM}^c . The explicit reference to, and integral over the breakup states, can be eliminated, using closure

$$\sum_{\sigma\mu} \int d\mathbf{k} |\phi_{\sigma\mu}^{(\pm)}(c, \mathbf{k}) \rangle \langle \phi_{\sigma\mu}^{(\pm)}(c, \mathbf{k})| = 1 - \sum_{i, M'} |\phi_{I'M'}^c(i) \rangle \langle \phi_{I'M'}^c(i)|, \quad (5)$$

where the sum on $i \equiv (n\ell j I)$ runs over *all* bound states $\phi_{I'M'}^c(i)$, having angular momentum structure $[(\ell' \times s)j' \times c]I'$, supported by the two-body potential which is used to bind the removed nucleon to the particular core configuration c in the initial state. This initial configuration is now denoted $i = 0$ and written $\phi_{IM}^c \equiv \phi_{IM}^c(0)$. The elastic breakup cross section is therefore

$$\sigma_{sp}(diff) = \frac{1}{2I+1} \int d\mathbf{b} \left[\sum_M \langle \phi_{IM}^c | |\mathcal{S}_c \mathcal{S}_n|^2 | \phi_{IM}^c \rangle - \sum_{i, M, M'} |\langle \phi_{I'M'}^c(i) | \mathcal{S}_c \mathcal{S}_n | \phi_{IM}^c \rangle|^2 \right]. \quad (6)$$

Replacing $\mathcal{S}_c \mathcal{S}_n \rightarrow (1 - \mathcal{S}_c \mathcal{S}_n)$ throughout simplifies the calculation, without change of value, provided the initial and final states in the original Eq. (4) are orthogonal. The two sets of terms are easily calculated and, since the \mathcal{S} are assumed spin independent

$$\begin{aligned} \langle \phi_{I'M'}^{c*}(i) | \phi_{IM}^c \rangle_{\text{spins}} &= \sum_{kq} (-)^{2s+2c+I+I'-\ell} \frac{\hat{\ell} \hat{\ell}' \hat{j} \hat{j}' \hat{I}}{\sqrt{4\pi}} (\ell 0 \ell' 0 | k 0) (I' M' k q | I M) \\ &\times W(j s k \ell'; \ell j') W(I c k j'; j I') u_{j' \ell'}^{c i}(r) u_{j \ell}^c(r) Y_{kq}(\hat{\mathbf{r}}), \end{aligned} \quad (7)$$

where the u^c are the bound state radial formfactors and Y_{kq} a spherical harmonic.

In analyses to date only the diagonal $i = 0$ term was retained in the second term in Eq. (6), the one bound state approximation, when

$$\langle \phi_{IM'}^c \phi_{IM}^c \rangle_{\text{spins}} = [u_{j\ell}^c(r)]^2 / 4\pi \delta_{MM'} \quad (8)$$

plus very small higher multipole (k) contributions when $\ell > 0$ and $I > 1/2$. This term clearly has a maximal radial overlap with the initial configuration. Also clear is that this truncation will, quite generally, overestimate the breakup since any additional bound state contributions will subtract cross section contributions. As well as being necessary for a complete description of the eikonal elastic breakup prediction, these extra matrix elements are precisely of the form of single-particle inelastic cross sections. Their magnitude therefore gives some indication of the expected cross sections for such processes and hence of the likely importance of single-particle excitation corrections to the spectator core model.

6. EIKONAL CALCULATIONS

In this Section we assess certain aspects of the accuracy of the calculations outlined, and their sensitivity to input parameters. We first assess those corrections due to the $i \neq 0$ bound state terms arising from the use of the closure relation in Eq. (6). For example in $^{11}\text{Be} \rightarrow ^{10}\text{Be}(\text{g.s.})$ the 2s-state binding potential also supports more deeply bound (nodeless) 1s- and 1p-states. The calculated corrections are, in total, only 0.5 mb. For $^{12}\text{Be} \rightarrow ^{11}\text{Be}(\text{g.s.})$ on the other hand, with radius and diffuseness parameters 1.25 and 0.7 fm, the 2s-state binding potential then also supports a weakly bound 1d-state ($S_n = 0.79$ MeV) and so the corrections are enhanced, to 4.2 mb. This compares with the total computed $\sigma_{sp} = 76$ mb. For $^{12}\text{Be} \rightarrow ^{11}\text{Be}(1/2^-)$ the well is shallower and the correction is 1.5 mb, while $\sigma_{sp} = 47$ mb. It is clear that if the effective potential supports near-threshold bound states, there can be non-negligible corrections from the $i \neq 0$ terms, and that it is therefore sensible to include these terms quite generally. They are expected in any case to be more important for heavier projectiles where the bound state level spacings are smaller and also more states contribute. More generally, the size of these corrections sets the scale (of order 1 mb) of cross sections for processes involving single-particle excitation in the projectile or the core at energies of 60–70 MeV/nucleon. These are seen to be small except in the special circumstances of coupling to a nearby and weakly-bound state. We contrast this with the likely magnitude of collective excitations. In the case of the weak $^{11}\text{Be} \rightarrow ^{10}\text{Be}(2^+)$ transition, a collective $0^+ \rightarrow 2^+$ contribution, of order 10 mb within the framework of the eikonal method, was needed to account for about half of the measured $^{10}\text{Be}(2^+)$ cross section [15]. In common therefore with what is known from transfer reactions, the most significant higher-order contributions in weak single-particle transitions are expected to arise from collective excitations, when such channels are available. Our limited experience suggests these are likely, typically, to be an order of magnitude greater than will arise from single particle excitations.

The calculations of Refs. [14–19] also use the optical limit (OL) form for the nucleon-target \mathcal{S}_n . This is less obviously valid for this partition at several 10's of MeV/nucleon. However, one finds [10], in the important surface region that the optical limit produces

an absorption profile $(1 - |\mathcal{S}_n(b_n)|^2)$ very similar to that calculated from the (better theoretically founded) effective nucleon-nucleus interaction of Jeukenne, Lejeune and Mahaux [25] (JLM). The latter, also calculated from the assumed target density, has been shown [26] to provide a good overall description of a large body of nucleon scattering data from light and medium mass nuclei at these energies. The latter \mathcal{S}_n is however, overall, more refractive and less absorptive than that of the optical limit. One finds as a result that, while the calculated total σ_{sp} are very similar (to within 10%), the division of this cross section between the stripping and breakup processes, shown as $(\sigma_{sp}(str), \sigma_{sp}(diff))$ mb, is somewhat different. The greater refraction and reduced absorption in the JLM case enhances the breakup cross section while reducing that for stripping. For example, for $(^{11}\text{Be}, ^{10}\text{Be}(\text{g.s.}))$ at 60 MeV/nucleon, the OL gives (124.7, 93.5) mb and the JLM (98.2, 127.8) mb. For $(^{12}\text{Be}, ^{11}\text{Be}(\text{g.s.}))$ at 78 MeV/nucleon, OL=(52.0, 23.8) mb and JLM=(40.6, 27.2) mb and for $(^{12}\text{Be}, ^{11}\text{Be}(1/2^-))$ the OL=(34.5, 12.7) mb and JLM=(28.7, 14.5) mb. Since the totals are the same to a reasonable precision, the two choices derive very similar spectroscopic factors from the eikonal calculations. Given the results of the following Section, where we find that fully quantum mechanical calculations of the breakup cross section generate a subtly different momentum distribution to that of the eikonal model, it may be possible to obtain an experimental handle on the relative magnitudes of the stripping and diffractive parts of the cross section even from these summed data. Of course, a measurement of the neutrons would, ideally, answer this question.

7. COUPLED CHANNELS ELASTIC BREAKUP CALCULATIONS

An assessment of the accuracy of the diffraction dissociation (elastic breakup) cross sections calculated using the eikonal description of the earlier section, and of the associated momentum distributions, can be made using fully quantum mechanical calculations in the case of the effective nucleon+core+target three-body problems we discuss here. While of greater complexity, these calculations have the advantage that they respect energy conservation and so can be used to examine results at a greater level of sophistication. Such a study is only really meaningful now that the different core state components of the cross section can be isolated as a result of the coincident photon measurements. Here we will compare the eikonal model predictions for the elastic breakup cross sections $\sigma_{sp}(diff)$ with those of coupled discretised continuum channels (CDCC) breakup calculations [27,28] for the $^{11}\text{Be}+^9\text{Be}$ system at 60 MeV/nucleon, the data for which are published [15].

In the CDCC the continuum of scattering states, in each significant I' spin-parity excitation of the two-body system, is divided into a number $\mathcal{N}(I')$ of representative energy intervals, usually referred to as momentum bins. For each such excitation interval i , $[k_{i-1} \rightarrow k_i]$, a square integrable wave function $u_\alpha, \alpha \equiv (i, (\ell's)j'cI')$ is constructed from the scattering states f_α in that interval by the superposition

$$u_\alpha(r) = \sqrt{\frac{2}{\pi N_\alpha}} \int_{k_{i-1}}^{k_i} g_\alpha(k) f_\alpha(k, r) dk, \quad (9)$$

where $g_\alpha(k)$ is a weight function, usually unity for a non-resonant continuum, and where

N_α is the normalisation

$$N_\alpha = \int_{k_{i-1}}^{k_i} [g_\alpha(k)]^2 dk \quad . \quad (10)$$

These bin states then act as effective discrete excited states of the core+nucleon system. The solution of the Schrödinger equation in this model space is then carried out by partial wave expansion and the solution of coupled equations. This bin state construction, and the resulting coupled channels calculations are implemented as an option in the versatile coupled channels code FRESKO [29] of Thompson. The outcome is a set of inelastic (two-body) transition amplitudes for exciting each of these continuum bins α , $T_{M'M}(\alpha, \mathbf{K}')$. These bin state inelastic amplitudes can then be used to compute the breakup amplitudes, to any given physical final state $\phi_\mu^{(+)}(c, \mathbf{k})$ of the core-nucleon system

$$\begin{aligned} T_{\mu\sigma;M}(\mathbf{k}, \mathbf{K}') &= \frac{(2\pi)^{3/2}}{k} \sum_{\alpha\nu} (-i)^\ell (\ell\nu\sigma\sigma|jm) (jmc\mu|I'M') \exp(i[\delta_\alpha(k) + \sigma_\ell(k)]) \\ &\times g_\alpha(k) Y_{\ell\nu}(\hat{\mathbf{k}}) T_{M'M}(\alpha, \mathbf{K}') \quad . \end{aligned} \quad (11)$$

Here \mathbf{K}' is the asymptotic wave number of the motion of the c.m. of the dissociated core and nucleon, $\delta_\alpha(k)$ is their relative motion phase shift in excitation state I' , and the sum is over all α such that $k \in \alpha$. Hence the laboratory triple differential cross sections for the nucleon and core fragments are obtained and, following integration over all directions of the unobserved nucleon, and over the perpendicular momentum components of the heavy residue, the parallel momentum differential cross section.

It is found that relative orbital angular momenta up to $\ell' = 5$ are needed to gain fully converged results for the $^{11}\text{Be} + ^9\text{Be}$ system at 60 MeV/nucleon. In each such angular momentum channel, typically $\mathcal{N}(I') = 10$ continuum bins were used, spanning nucleon-core relative motion excitation energies from zero to 20 MeV. The interaction describing this relative motion in the continuum states was taken to be that which binds the ^{11}Be ground state, as in the eikonal calculations. Similarly, to compare with the eikonal results for the integrated $\sigma_{sp}(\text{diff})$, the JLM neutron-target interaction and the strongly absorptive potential corresponding to the optical limit \mathcal{S}_c for the core-target system, were used to compute the required bound-continuum and continuum-continuum coupling potentials.

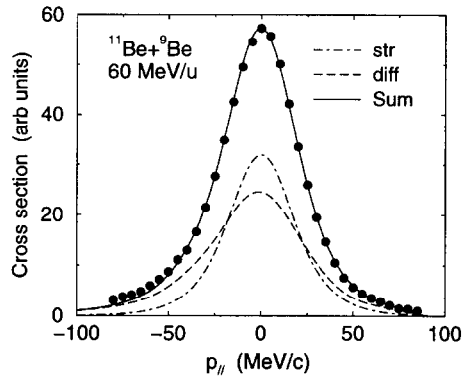


Figure 1. Calculated (CDCC) elastic breakup and (eikonal) stripping contributions to the $^{10}\text{Be}(\text{g.s.})$ parallel momentum distribution, for $^{11}\text{Be} + ^9\text{Be}$ at 60 MeV/u, and their sum. The solid points are the data from Ref. [15].

The calculated $\sigma_{sp}(diff)$ from the coupled channels calculations, 120.8 mb, is in rather good agreement with that from the (JLM) eikonal calculation, given earlier as 127.8 mb. However, in Figure 1 the distribution of the residue's cross section with the parallel momentum is distinctly different. In the eikonal model the parallel momentum distribution for the breakup component is predicted to be the same as that for the stripping part [30], and symmetric. This was assumed in all earlier analyses, e.g. [15]. The dashed line in Figure 1 shows the fully quantum mechanical calculation to be asymmetric, with a low energy tail. This reflects the redistribution of energy from centre of mass motion to internal excitation of the projectile - treated correctly in the coupled channels calculations. The solid curve results when the stripping and diffraction cross sections are added, such that they make equal contributions, as suggested by the eikonal model calculations. The solid points are the data, taken from Ref. [15]. The asymmetry in the data is very satisfactorily reproduced by the enhanced calculations.

In Figure 2 the distribution of the cross section with the parallel momentum of the $^{10}\text{Be}(g.s.)$ residue, from the CDCC calculation, is now shown as a function of the half angle of the acceptance cone of the detected residues about the incident beam direction. It is clear that the momentum distribution changes characteristically as a function of the acceptance. The distribution becomes broader and the peak moves to lower momentum with increasing momentum bite. This effect is seen more clearly if one calculates the cross sections for residues emerging in different annular bins. In cases where the statistics allow such a decomposition of the data also, this promises an additional diagnostic tool in understanding the data and its division between the breakup and stripping mechanisms.

We find that, for $^{10}\text{Be}(g.s.)$ residues emerging in the laboratory frame at angles beyond 2.5° , the measured cross sections can be accounted for entirely by those elastic breakup events calculated using the CDCC. We therefore compare these events assuming they arise from the diffraction dissociation mechanism only. The momentum distribution of these experimental events (solid points) are shown in Figure 3, for residues in the range 2.5° – 3.0° . Data in larger angle intervals show very similar features, the data getting smaller, broader, and with a greater shift in the peak position with angle.

The solid curve is the calculated CDCC prediction. The dashed curve shows, for comparison, the shape of the momentum distribution measured in events only at the most forward angles 0° – 0.5° , and which is in perfect agreement with the momentum distribution predicted using the eikonal theory, Figure 4. The broadening and shift in peak position of the distribution with residue detection angle is revealed and also nicely described. The CDCC calculation tracks this behaviour also in the higher angle cuts.

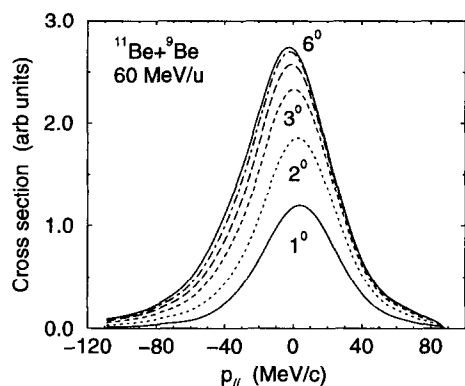


Figure 2. Calculated (CDCC) elastic breakup contributions to the $^{10}\text{Be}(g.s.)$ parallel momentum distribution, for $^{11}\text{Be} + ^9\text{Be}$ at 60 MeV/u as a function of the acceptance angle of the ^{10}Be residues.

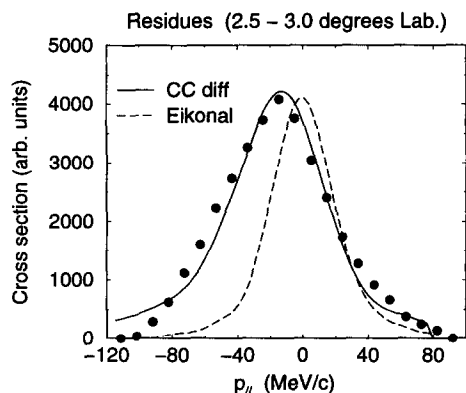


Figure 3. Calculated (CDCC) and experimental elastic breakup contributions to the $^{10}\text{Be}(\text{g.s.})$ parallel momentum distribution, for residues in the range 2.5° – 3.0° .

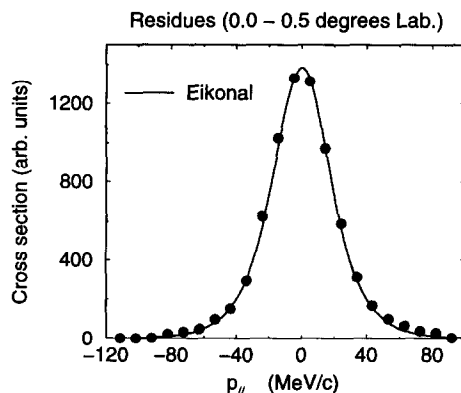


Figure 4. Calculated eikonal and experimental elastic breakup contributions to the $^{10}\text{Be}(\text{g.s.})$ parallel momentum distribution, for residues in the range 0.0° – 0.5° .

These calculations reinforce the view that the reaction mechanism, and the extraction of the ground state component from the data, since the ground state cross section requires a subtraction of those events in which a photon is observed, are well understood. Further work will be carried out on this and the ^{15}C induced reaction.

8. SUMMARY AND OUTLOOK

In this paper we have reviewed the assumptions which underpin present eikonal calculations of single-nucleon knockout reactions. These have shown considerable promise for carrying out efficient spectroscopy of strong single-particle states, even for very rare isotope beams, at fragmentation energies. We have also presented general estimates of the likely cross sections for collective and single-particle inelastic excitations which will be the leading order corrections to the spectator core model. It is expected that, as in transfer reaction studies, the surface dominance of the reaction and surface peaking of collective transition formfactors mean that collective excitations will dominate in cases where such channels are present. A ball-park figure for inelastic single-particle effects is of order 1 mb at energies of excess of 60 MeV. These can be larger for very weakly bound states. These corrections may be important if it is necessary to understand, in specific cases, weaker transitions and the population of configurations with otherwise small single-particle spectroscopic strength.

Regarding the accuracy of the spectator core model calculations themselves, the eikonal elastic breakup calculations have also been generalised to include all of the bound state terms which result from our use of the closure relationship over breakup states. In general their contributions are small in the light systems studied to date. Their inclusion is expected to be more important with increasing projectile mass. The sensitivity of the calculations to the assumed removed-nucleon target interaction is also quantified. The optical limit and JLM generated neutron profile functions, both derived from a target

matter density approach, calculate cross sections which differ by less than 10%, although the balance between the stripping and elastic breakup mechanisms is more different. These effects do not therefore have any significant implications for the deduced spectroscopy and its successful comparison with the shell model in analyses to date.

An outstanding difference between the experimental and eikonal model predictions of the parallel momentum distribution, a significant asymmetry and a low momentum tail observed in the distribution of ground state residues in knockout from the ^{11}Be and ^{15}C systems, is also investigated. We show that fully quantum mechanical calculations of the elastic breakup component of the cross section, using the discretised continuum coupled channels method, are able to explain this effect and so confirm and give confidence in the basic reaction mechanisms being used. It is shown that the angular distribution of these residues, equivalent to the distribution of cross section with their perpendicular momentum component, could be used to study this mechanism in more detail. Since the observed asymmetry does not affect the extraction of the neutron ℓ -value from the data and the elastic breakup cross section obtained using the improved calculations is in agreement with that from the eikonal model, there are no spectroscopic implications from this clarification. These calculations and data may however permit a clarification of the division of cross section between the stripping and diffraction dissociation mechanisms.

The author would like to acknowledge the on-going collaboration with colleagues at Michigan State University which has stimulated and progressed this work. The advice of Ian Thompson on the details of the implementation of the CDCC method within FRESKO is gratefully acknowledged. I thank also Daniel Bazin for providing the preliminary angular decomposition of the ^{11}Be knockout data shown in Figures 3 and 4.

REFERENCES

1. R.J. Glauber, in *Lectures in Theoretical Physics*, ed. by W.E. Brittin (Interscience, New York, 1959), Vol. 1, p315.
2. K. Hencken, G.F. Bertsch, and H. Esbensen, Phys. Rev. C 54 (1996) 3043.
3. G.F. Bertsch, K. Hencken and H. Esbensen, Phys. Rev. C 57 (1998) 1366.
4. A. Bonaccorso and D.M. Brink, Phys. Rev. C 58 (1998) 2864.
5. C.A. Bertulani and H. Sagawa, Nucl. Phys. A588 (1995) 667.
6. K. Yabana, Y. Ogawa and Y. Suzuki, Phys. Rev. C 45 (1992) 2909; Nucl. Phys. A 539 (1992) 295.
7. J.S. Al-Khalili, I.J. Thompson and J.A. Tostevin, Nucl. Phys. A 581 (1995) 331.
8. J.A. Tostevin, J.S. Al-Khalili, M. Zahar, M. Belbot, J.J. Kolata, K. Lamkin, D.J. Morrissey, B.M. Sherrill, M. Lewitowicz, and A.H. Wuosmaa, Phys. Rev. C 56 (1997) R2929.
9. P.G. Hansen, Phys. Rev. Lett. 77 (1996) 1016.
10. J.A. Tostevin, in: 'Fission and Properties of Neutron-rich Nuclei', Proceedings of the Second International Conference (St Andrews, Scotland, 28 June - 3 July 1999) ed. by J.H. Hamilton, W.R. Phillips and H.K. Carter, World Scientific (Singapore), March 2000, 429.
11. N.K. Glendenning, in Nuclear Spectroscopy and Reactions, Vol. D, ed J. Cerny, Academic Press, 319.

12. P.G. Hansen, J. Phys. G 25 (1999) 727.
13. J.A. Tostevin, J. Phys. G 25 (1999) 735.
14. A. Navin *et al.*, Phys. Rev. Lett. 81 (1998) 5089.
15. T. Aumann *et al.*, Phys. Rev. Lett. 84 (2000) 35.
16. A. Navin *et al.*, Phys. Rev. Lett., 85 (2000) 266.
17. V. Guimarães *et al.*, Phys. Rev. C 61 (2000) 064609.
18. A. Navin *et al.*, Proc. Int. Conf. on experimental nuclear physics in Europe (ENPE99) (Seville, June 21–26 1999) ed B. Rubio and W. Gelletly, AIP Conf. No. 495 (AIP New York 1999), 309.
19. V. Maddalena *et al.*, “Single-nucleon knockout reactions: Application to the spectroscopy of $^{16,17,19}\text{C}$ ”, Phys. Rev. C, submitted, Preprint MSUCL-1171, August 2000.
20. E. Sauvan *et al.*, “One-neutron removal reactions on neutron-rich *psd*-shell nuclei”, Phys. Lett. B, submitted.
21. H. Sagawa and Y. Yazaki, Phys. Lett., B244 (1990) 149.
22. M. Hussein and K. McVoy, Nucl. Phys. A445 (1985) 124.
23. M. Ichimura, Int. Conf. on Nuclear Reaction Mechanism (Calcutta, January 3–9 1989) ed S. Mukherjee, World Scientific (Singapore), 374.
24. S. Kox *et al.*, Phys. Rev. C 35 (1987) 1678.
25. J.-P. Jeukenne, A. Lejeune, and C. Mahaux, Phys. Rev. C 16 (1977) 80.
26. J.S. Petler, M.S. Islam, R.W. Finlay, and F.S. Dietrich, Phys. Rev. C 32 (1985) 673; S. Mellema, R.W. Finlay, F.S. Dietrich, and F. Petrovich, Phys. Rev. C 28 (1983) 2267.
27. M. Kamimura *et al.*, Prog. Theor. Phys. Suppl. 89 (1986) 1.
28. N. Austern *et al.*, Phys. Rep. 154 (1987) 125.
29. I.J. Thompson, Comp. Phys. Rep. 7 (1988) 167;
FRESCO users’ manual, University of Surrey, UK.
30. F. Barranco and E. Vigezzi, *International School of Heavy-Ion Physics, 4th Course: Exotic Nuclei*, ed. by R.A. Broglia and P.G. Hansen (World Scientific, Singapore, 1998) p217.